Elasticity driven self-organization of polarons

P. Maniadis, T. Lookman, and A. R. Bishop
Theoretical Division and Center for Nonlinear Studies, Los Alamos National Laboratory, Los Alamos, New Mexico 87545, USA
(Received 5 August 2008; published 17 October 2008)

We use a strain description to couple long-range elastic fields adiabatically to electronic density to describe the behavior of a quantum particle in an elastic medium. We show that in this generalization of the Holstein polaron problem, a bound polaronic state results with strong long-range angular dependence in the elastic fields, but a localized electronic core. The deformation of the elastic fields creates an anisotropic, indirect interaction between polarons extending to large distances. For a given density of polarons, this interaction favors the formation of strings of polarons in preferred directions.

DOI: 10.1103/PhysRevB.78.134304 PACS number(s): 62.20.−x, 71.38.Ht, 63.20.Pw

Intrinsic multiscale heterogeneities from nanoscales to mesoscales result from the coupling of strain or lattice distortions with spin and charge. They have been studied by fine-scale microscopies in, e.g., many complex oxide materials, including cuprates, manganites, and magnetoelectrics.[1–4] Various *cross-variable* responses occur in the presence of external fields, e.g., magnetic fields can switch electric polarization[5] in magnetoelectrics and resistivity can fall drastically, both in a magnetic field (colossal magnetoresistance[6]) and under applied stress (colossal stressoresistance[7]). The responses are also *cross scale*, with *nanoscale* metallic percolativity controlled by the strength of a *uniform* magnetic field or applied stress.[8] Clearly, an understanding of this multivariable, multiscale patterning or texturing is central to understanding how complex material functionalities may be tailored.

It has become increasingly clear that such patterning can arise from a competition between short- and long-range forces.[1–4] These forces include those due to electron-lattice coupling, the Coulomb interaction, and strain mediated forces. They have been invoked, for example, in understanding the formation of "stripes" in cuprates,[9] as well as the formation of bipolaronic or multipolaronic states due to the lattice deformation accompanying doped charges.[10] It has also been shown how stringlike multipolaronic patterns can result from competing Coulomb and electron-lattice interactions.[11] Stripe segments have also been observed in colossal magnetoresistance materials with STM. The theoretical treatments have predominantly been based on many-body considerations with the lattice included through the hopping strength or as a single variable displacement field. Our objective here is to consider the interaction of the charge in the lattice through a strain field, which serves as the appropriate lattice order parameter, so that intermediate-range anisotropic elastic correlations may be taken into account. This has usually been left implicit in many earlier treatments,[12] and the effects of the strain mediated anisotropy on the electronic properties has not been addressed. Thus, for example, the stringlike polarons previously considered do not have any directional dependence.

Our work can also be viewed as a generalization of the semiclassical anharmonic Holstein polaron model with an on-site potential.[13–15] The coupling to the lattice in these models is via a one-component displacement field that couples to the electronic density. We suggest that the long-range strain fields serve as the natural elastic order parameters that couple to the electronic density; we therefore explore how these anisotropic strain fields affect the stationary properties of the polaron. In particular, we study the potential for induced anisotropy of the electronic density due to the strains in a two-dimensional (2D) elastic medium, and show how the electron localization is affected by the elastic properties of the medium.

Our work represents an application of tools developed for strain-based materials, such as martensites and ferroelectrics, where explicit long-range interactions that arise as a result of satisfying fundamental bonding constrains, are incorporated.[16] Our main results show than the long-range interactions favor the formation of polaron strings in certain preferred directions. In contrast to the coupling of strain to a classical particle where the density follows the angular strain dependence,[3] we find that the self-consistent solution involving the Schrödinger equation for the particle, considerably localizes the polaron with a very weak-anisotropy induced from the strain field.

In Sec. II we describe our strain-polaron model in 2D and derive the effective eigenvalue problem for the electronic density. In Sec. III we discuss how the polaron energy varies with the electron-lattice coupling for different elastic stiffnesses. Of particular interest here is the variation in the coupling parameter threshold value with elastic properties. In Sec. IV we generalize our model to a finite density of polarons and study configurations of polarons which minimize the energy for a given polaron density.

I. STRAIN DESCRIPTION OF POLARONS IN AN ELASTIC MEDIUM

The symmetry adapted, principal strains for a two-dimensional square lattice can be written as

$$e_1 = \frac{1}{\sqrt{2}}(\epsilon_{xx} + \epsilon_{yy}); \quad e_2 = \frac{1}{\sqrt{2}}(\epsilon_{xx} - \epsilon_{yy}); \quad e_3 = \epsilon_{xy} = \epsilon_{yx}, \tag{1}$$

where e_1 is the compressional (or dilatational) strain, e_2 the deviatoric strain and e_3 the simple shear strain associated with a unit cell. In the small strain approximation, which we will restrict ourselves to, the Lagrangian strains, ϵ_{ij}, are defined by

$$\epsilon_{ij} = \frac{1}{2}\left(\frac{\partial u_i}{\partial x_j} + \frac{\partial u_j}{\partial x_i}\right),$$

where u_i, $i=1,2$ are the two displacements in the x and y directions of the 2D lattice. The three strains in 2D are not all independent and are related in a defect-free medium by the integrability or St. Venant compatibility constraint (in general $\nabla \times \nabla \times \vec{\vec{\epsilon}} = 0$)

$$\partial_x^2 \epsilon_{yy} + \partial_y^2 \epsilon_{xx} - 2\partial_x \partial_y \epsilon_{xy} = 0,$$

which in terms of the symmetry adapted strains becomes

$$G = (\partial_x^2 + \partial_y^2)e_1 - (\partial_x^2 - \partial_y^2)e_2 - \sqrt{8}\partial_x \partial_y e_3 = 0.$$

The displacements can be obtained as derived variables (within an arbitrary constant) from strain using the Fourier space relations

$$u_x(\vec{k}) = \frac{1}{i\sqrt{2}K_x}[e_1(\vec{k}) + e_2(\vec{k})]; \quad u_y(\vec{k}) = \frac{1}{i\sqrt{2}K_y}[e_1(\vec{k}) - e_2(\vec{k})]. \tag{2}$$

Although the shear strain $e_3(\vec{k})$ does not appear explicitly above, it is related to $e_{1,2}(\vec{k})$ via the compatibility constraint.

The elastic energy density for a homogeneous medium is given by Hooke's law

$$F_{el} = \frac{A_1}{2}e_1^2 + \frac{A_3}{2}e_3^2 + \frac{A_3}{2}e_3^2,$$

where A_1, A_2, and A_3 are the elastic moduli and the three strains are independent. If a quantum particle is introduced in the lattice, it will be coupled to the deformations of the elastic fields. The model we use for the description of the particle and its interactions with the elastic fields is an extension of the semiclassical Holstein polaron model.[13] The interaction is described by the Hamiltonian interaction density

$$H_{\text{int}} = \chi|\Psi|^2 e_1, \tag{3}$$

where Ψ is the wave function of the particle and e_1 is the isotropic, dilatational strain mode. We treat the system in the semiclassical approximation with the elastic fields treated classically and the particle quantum mechanically. The Schrödinger equation describing the particle in the presence of the elastic field can be written as

$$i\frac{d\Psi}{dt} = -V\nabla^2\Psi + \chi e_1 \Psi, \tag{4}$$

where we choose the Planck constant, $\hbar = 1$ to rescale time. For the derivation of the above equation we considered the kinetic energy of the quantum particle. We also assumed that, in the Born-Oppenheimer approximation, the wave function of the particle does not depend explicitly on the elastic fields. The Schrödinger equation we derived for the wave function is of the form $i\frac{d\Psi}{dt} = \hat{H}_e\Psi$, where $\hat{H}_e$ represents the quantum particle component of the Hamiltonian

$$\hat{H}_e = -V\nabla^2 + \chi e_1. \tag{5}$$

For large χ, the interaction of the particle with the elastic substrate creates a localized polaronic state, whereby there is a localized deformation of the field e_1 by the electronic density. This leads to a bound state with energy lower than the extended plane-wave energy band, and this self-sustained bound state becomes the ground state of the system. Since the polaron is an eigenstate of the quantum problem, we assume that Ψ is stationary, i.e., the time evolution of the wave function is given by the expression $\Psi(\mathbf{r},t) = \Phi(\mathbf{r})\exp(-iEt)$. In the adiabatic approximation limit, we assume that the lattice relaxes fast enough that it is effectively "slaved" to changes in the electronic density of the quantum particle.

The localized deformation of the elastic fields can be calculated self-consistently by assuming an initial localized wave function Ψ and then minimizing the elastic energy together with the interaction. The energy functional that we minimize is

$$\int d\mathbf{r}\{F_{el} + H_{\text{int}} + \Lambda G\}, \tag{6}$$

where, with the introduction of the Lagrange multiplier Λ, we ensure that the elastic fields e_1, e_2, and e_3 will be consistent with the compatibility constraint, $G=0$, in order to allow for inhomogeneous deformations of the medium. As we have chosen e_1, the dilational-compressional mode, to couple to the electronic density, it is convenient to consider it as an order parameter (OP). The minimization of the energy functional (6) with respect to the elastic fields e_2 and e_3 leads to:

$$A_2 e_2 - (\nabla_x^2 - \nabla_y^2)\Lambda = 0 \Rightarrow e_2(\vec{k}) = \frac{1}{A_2}(k_x^2 - k_y^2)\Lambda(\vec{k}) \tag{7}$$

$$A_3 e_3 - \sqrt{8}\nabla_x \nabla_y \Lambda = 0 \Rightarrow e_3(\vec{k}) = \frac{\sqrt{8}}{A_3}k_x k_y \Lambda(\vec{k}). \tag{8}$$

We have transformed the fields into Fourier space, as the algebraic equations are then easier to handle. By requiring $e_2(\vec{k})$ and $e_3(\vec{k})$ to satisfy the compatibility constraint, the Lagrange multiplier, Λ, is expressed in terms of $e_1(\vec{k})$:

$$\Lambda(\vec{k}) = \frac{A_2 A_3 k^2}{8A_2 k_x^2 k_y^2 + A_3(k_x^2 - k)y^2)^2} e_1(\vec{k}) \tag{9}$$

and the minimization of Eq. (6) with respect to e_1 yields

$$e_1(\vec{k}) = -\chi\{|\Psi|^2\}_k \frac{A_3(k_x^2 - k_y^2)^2 + 8A_2 k_x^2 k_y^2}{A_2 A_3 k^4 + 8A_1 A_2 k_x^2 k_y^2 + A_1 A_3 (k_x^2 - k_y^2)^2}. \tag{10}$$

The notation $\{|\Psi|^2\}_k$ describes the spatial Fourier transform of the probability density $|\Psi|^2$. A calculation of the elastic energy F_{el} shows that eliminating the compatibility constraint in Eq. (5) leads to an anisotropic long-range interaction of the form $\sim\frac{\cos(4\theta)}{r^2}$ (were θ is the polar angle of the wave-vector $\vec{k}$) with the anisotropy reflecting the discrete symmetry encoded in the strains due to the square unit cell. Thus, e_1 in Eq. (10) results from the coupling of the electronic density to the spatially long-range interactions arising from the elastic degrees of freedom in this *strain only* OP-

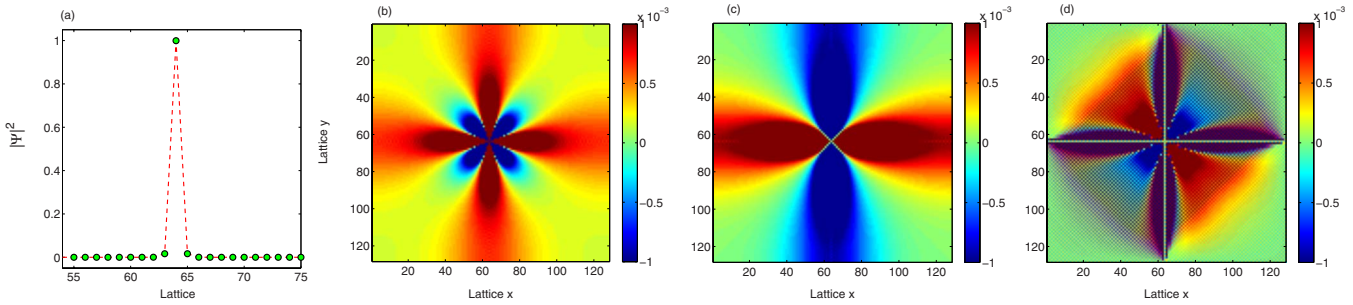

FIG. 1. (Color online) The polaron with elastic constants $A_1=A_2=A_3=1$: (a) cross section of the probability density $|\Psi|^2$ showing that the polaron is well localized; (b) the compressional-dilational e_1 $[=\frac{1}{\sqrt{2}}(\epsilon_{xx}+\epsilon_{yy})]$ field; (c) the deviatoric strain e_2 $[=\frac{1}{\sqrt{2}}(\epsilon_{xx}-\epsilon_{yy})]$ field; (d) the simple shear e_3 $(=\epsilon_{xy})$ field.

based picture, in contrast to the prevalent displacement-based approaches to the polaron problem.

The existence of the shear strain, e_3, in the expression for the elastic energy is important for the description of the angular dependence of the polaron strain fields. If the shear strain is discarded, the energy density reduces to $F_{el}=F_1(e_1)+F_2(e_2)$, where F_1 and F_2 are chosen to be harmonic but which can be generalized to any physically acceptable nonlinear energy function. It can be shown that in this case the description of the semiclassical Holstein model becomes equivalent to the simple two-dimensional Holstein problem studied in Ref. 13, where the on-site potential of each lattice site is not harmonic (similar polarons with anharmonic on-site potential have been studied in Refs. 14 and 15). The variable that is important in this case (in the displacement representation) is the displacement u along the diagonal of the lattice (the displacements in the x and y directions are forced to be equal, and therefore only one variable is sufficient to describe the system). When we introduce the shear strain in our model, the compatibility condition breaks constraints between the displacements along the x and the y directions and the displacements are not forced to be equal. From this we conclude that the three fields (e_1, e_2, and e_3), together with the compatibility condition, provide the minimum requirements for the description of a 2D elastic polaron.

For the numerical investigation of the polaron properties we use the Aubry method (for details see Ref. 13). The basic idea of this method is that when the Hamiltonian is applied on an initial guessed wave function Ψ, and the result is normalized, the process will converge to the ground state if applied several times. This method is very efficient and it converges to the polaron solution with an accuracy of the order of 10^{-10}. We choose a lattice size 128×128 on which the spatial derivatives of the wave function are discretized. We start with a delta function at the center of the lattice as an initial guess to the wave function. The elastic field, e_1, is calculated using expression (10). For the next step we apply the Aubry method, using e_1, and we calculate the next iteration to the wave function. We repeat this process until we achieve the solution with the desired accuracy. Together with the wave function, we calculate the electronic part of the energy, which is the eigenvalue of the Hamiltonian

$$E\Psi=\hat{H}_e\Psi. \tag{11}$$

II. ONE POLARON RESULTS

The exponential decay of the electronic density $|\Psi|^2$ is very rapid and as a result it remains well localized at the center of the lattice. On the other hand the deformations of the elastic fields extend far from the center of the polaron (Figs. 1 and 2). From expression (10) that connects the elastic fields and the electronic probability, we expect to have some angular dependence of the polaron. However, this angular dependence of the probability distribution is found to be very weak—at least four orders of magnitude smaller than the exponential decay.

From Eq. (10) we see that the angular dependence disappears when $A_3=2A_2$ and for any value of A_1 [this can be seen if we substitute the wave vectors in Eq. (10) in polar coor-

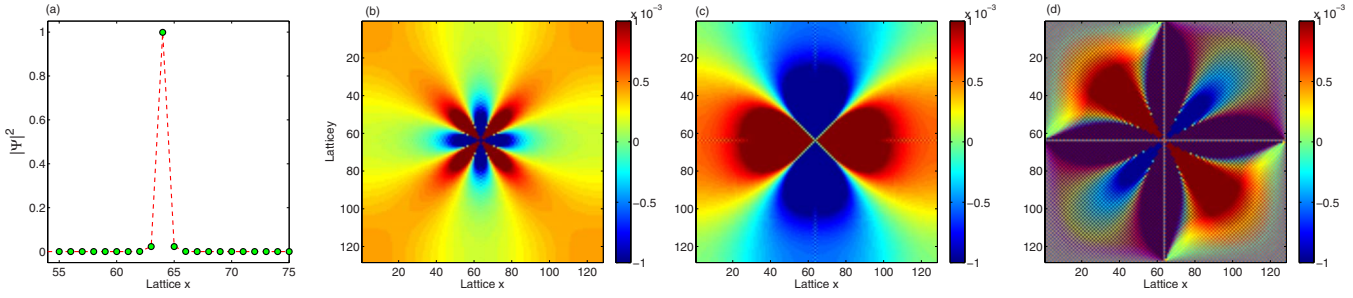

FIG. 2. (Color online) The polaron with elastic constants $A_1=A_2=1$ and $A_3=3$: (a) cross section of the probability density $|\Psi|^2$; (b) the e_1 field; (c) the e_2 field; (d) the e_3 field.

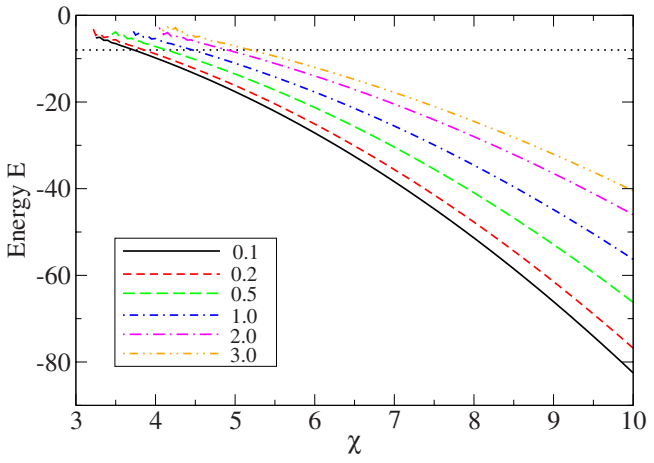

FIG. 3. (Color online) The electron energy E as a function of the coupling parameter χ for $A_1=A_2=1$ and for $A_3=0.1,0.2,0.5,1.0,2.0,3.0$. The dotted horizontal line is the edge of the extended band states. The polaron becomes metastable when the energy E enters the band.

dinates]. We used the parameters $A_1=A_2=1$ and $A_3=1,2$ to calculate polarons with the same exponential decay with and without angular dependence. From comparing these two cases, we have been able to estimate the difference, from which we find the angular dependence of the probability distribution $|\Psi|^2$ to be approximately 4 orders of magnitude smaller than the exponential decay.

Using the above numerical technique, we were able to verify the results presented in Ref. 13 when the shear strain is eliminated. In Fig. 3 we present the electron energy E [calculated using Eq. (11)] as a function of the coupling χ and for different values of the shear coefficient ($A_3=0.1,0.2,0.5,1.0,2.0,3.0$). We have been able to numerically find the polarons for a large range of parameters. As the coupling χ decreases, the energy E enters the band of the extended states. At this critical value of the coupling, the polaron becomes unstable. Varying the strength of the shear strain A_3 we see that the energy E decreases, and therefore the critical value of the coupling increases.

By comparing Figs. 1(b) and 2(b) we see that the angular dependence of the e_1 field is rotated by $\pi/4$ when the shear strain contribution in the free energy A_3 becomes larger than $2A_2$. For $A_3<2A_2$ the angular dependence of the e_1 field is such that the field has maxima along the main directions, while it has minima along the diagonals. For $A_3=2A_2$ the angular dependence disappears, and for $A_3>2A_2$ the picture is reversed; the field e_1 has minima along the main lattice directions, and maxima along the diagonals. This will affect the ordering directions of the many-polaron stripe formation on the lattice, as shown next.

III. MANY POLARON FORMALISM

We have seen in the previous section that the elastic fields extend to relatively large distances from the center of the polaron and also preserve the proper symmetry and angular dependence. This leads to the expectation that the elastic substrate should mediate an effective long-range interaction between polarons that would otherwise be too widely separated to interact through a screened Coulomb interaction. We therefore consider a number of independent quantum particles in the computational system, where each particle is described by its own wave function Ψ_i. We also assume that there is a hard-core interaction between the particles described by the Hamiltonian

$$H_c = \sum_{i,j} u_0 |\Psi_i|^2 |\Psi_j|^2, \tag{12}$$

with the parameter u_0 determining the strength of the local interaction, for which we choose a value between 4 and 10, large enough to create an energy barrier for two particles to be located at the same lattice site.

The Schrödinger equation for each particle takes the form

$$i\frac{d\Psi_i}{dt} = -V\nabla^2\Psi_i + \chi e_1 \Psi_i + u_0 \sum_{j\neq i} |\Psi_j|^2 \Psi_i, \tag{13}$$

where now the interaction between the particles and the elastic fields is assumed to be a superposition over all the polarons,

$$H_{\text{int}} = \chi \sum_i |\Psi_i|^2 e_1,$$

so that the strain e_1 is given by

$$e_1(\vec{k}) = -\chi \left\{ \sum_i |\Psi_i|^2 \right\}_k \frac{A_3(k_x^2-k_y^2)^2 + 8A_2k_x^2k_y^2}{A_2A_3k^4 + 8A_1A_2k_x^2k_y^2 + A_1A_3(k_x^2-k_y^2)^2}. \tag{14}$$

Using this formalism, we explore the properties of the system with more than one polaron. We start with the simple case of two polarons, and study the indirect interaction between them due to the long-range deformation of the elastic substrate. In Fig. 4 we plot the elastic fields e_1, e_2, and e_3 when the distance between the two polarons is $(l_x,l_y)=(20,20)$ lattice sites. The exponential localization of the wave function of both polarons is very strong, and therefore there is no direct interaction between the two wave functions. However, as we can see in Fig. 4, the elastic fields have a much longer range, and as a result, there is an interaction between the polarons. The existence of the first polaron creates deformations in the elastic fields, which extend for a long distance, making it easier or more difficult for the second polaron to deform the fields, depending on both the distance as well as the orientation. In Figs. 5(a) and 5(b) we show the energy of the system as a function of the position of the second polaron, assuming that the first polaron is located at the center of the lattice. The parameters we use in this system are $A_1=A_2=A_3=1$ and $\chi=4.0$. As we can see, there is an energy barrier at the center which means that the two polarons cannot overlap. The barrier extends along the main directions of the lattice for a relatively large distance. On the other hand, there are four minima along the diagonals, and at a very close distance to the center. This means that the two polaron system will minimize its energy when the two polarons are close, and their relative position is in accordance

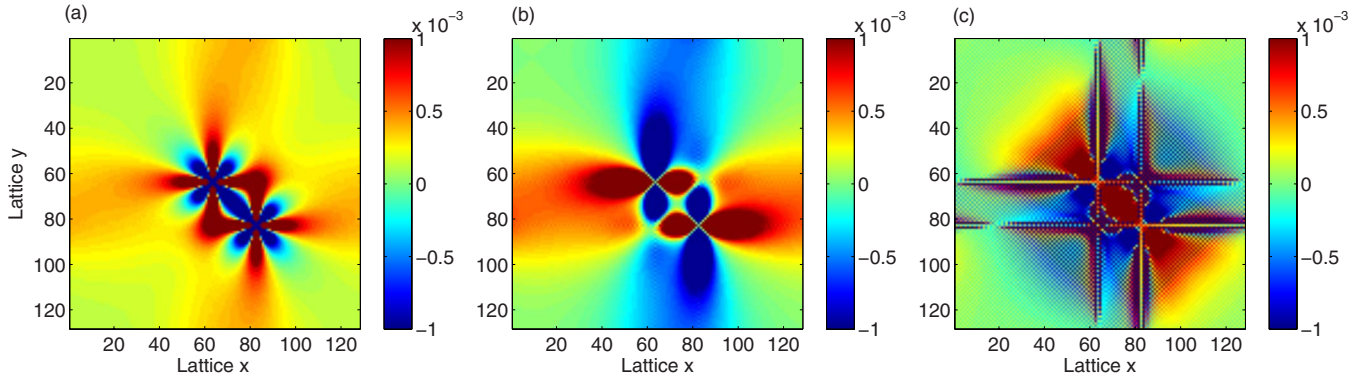

FIG. 4. (Color online) The strain fields for two polarons with elastic constants' $A_1=A_2=A_3=1$: (a) the e_1 field; (b) the e_2 field; (c) the e_3 field.

with the symmetry of the order-parameter fields (which in this case is e_1). The angular dependence of the field is reflected in this way in an energy landscape in terms of the relative distance and orientation of the two polarons.

The local minima of the interaction energy in Figs. 5(a) and 5(b), are along the diagonal for $A_3<2A_2$ as we expect, because, for this parameter range, the deformation of the e_1 field has a minimum along the diagonal, making it easier to arrange many polarons in this direction. If we increase A_3 when it becomes larger than $2A_2$, there is a rotation by $\pi/4$ and the minima e_1 are along the main directions of the lattice. Due to this rotation, there is a similar rotation in the directions of the interaction energy. For $A_e>2A_2$ we find that the minimum of the interaction energy is along the main directions of the lattice. The parameters A_1, A_2, and A_3 can be calculated from the elastic constants for real materials, and they have a linear temperature dependence. We have found that for a given material the transition from the $A_3<2A_2$ to the $A_3>2A_2$ situation can take place for temperatures $\sim T=400$ °K (Ref. 17) (for Fe with 30% Pd).

We now continue exploring the dynamics of the multipolaron system by introducing a third polaron. We focus on the case where $A_3<2A_2$; the results are the same for $A_3>2A_2$ with a $\pi/4$ rotation. Since the two polaron system has an energy minimum when the two particles are close to each other and along the diagonal, we keep this arrangement and add a third particle. We move the particle on the lattice and we calculate the energy of the system as a function of its distance and orientation with respect to the two other polarons [Figs. 5(c) and 5(d)]. We see that the barrier in the main directions of the lattice and the minima along the diagonals remains, but there are some differences. The two polarons, already placed at the center, occupy one of the two diagonals. The minima along this diagonal are slightly amplified due to the constructive contribution of the two particles. At the same time, due to the destructive contribution of the barriers, the minima along the other diagonal become weaker.

It is clear from the analysis of the energy landscape that when the number of polarons is small compared to the size of the system, then the angular dependence of the elastic field will favor the creation of a single string of polarons along the diagonal. We have confirmed this by calculating the energy of different configurations. In Table I we present the energy per polaron (the total energy divided by the number of polarons) for the four arrangements shown in Fig. 6, and for $N_p=20$ and $N_p=32$ polarons on the lattice

When the number of particles is small, the ground state will correspond to the state where all of the particles are located along one of the diagonals. We wish to see what happens when the number of particles is large compared to the size of the system. In this case, we expect that a fraction

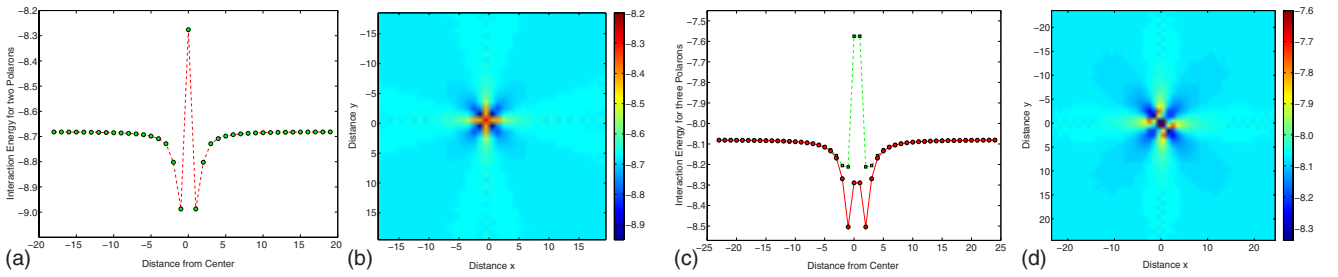

FIG. 5. (Color online) (a) Interaction energy profile along the diagonal for two interacting polarons as a function of their distance for $A_1=A_2=A_3=1$. One polaron is kept at a fixed position, at the center of the lattice, and we calculate the energy of the system as a function of the distance to the second polaron. Points are numerical data and the line is a guide to the eye. (b) Density plot of the same interaction energy as in (a). (c) Interaction energy for three polarons as a function of their distance for $A_1=A_2=A_3=1$. Two polarons are located at the center but along the $x=-y$ diagonal. We calculate the energy of the system as a function of the distance of the third polaron from the other two. The continuous line and circles are for the diagonal $x=-y$, whereas the dashed line and squares are for the third polaron along the other diagonal $x=y$. (d) Density plot of the same interaction energy as in (c).

TABLE I. The energy per polaron, for $N_p=20$ and $N_p=32$, corresponding to the four arrangements shown in Fig. 6.

	$N_p=20$	$N_p=32$
a	−3.075	−3.096
b	−3.009	−3.051
c	−2.961	−3.021
d	−2.953	−3.007

of the particles will form a string along the diagonal, and the rest will arrange themselves to minimize the energy. Due to the nature of the hard-core interactions we cannot consider a very large number of particles. To mitigate this limitation, we decrease the size of our lattice to 55×55. When we put a commensurate number particles on the lattice ($N_p=55$), we find that the minimum of the energy occurs when all of them are arranged along the diagonal with an energy per particle $E_p=-5.7603$. For the same number of particles we find slightly higher energies if we place them in two parallel stripes ($E_p=-5.5871$) or in an "*X* pattern" similar to Fig. 6(c), yielding $E_p=-5.5776$.

When we add one more particle, the lowest energy is achieved when the diagonal is fully filled and the extra particle is placed in one of the minima that appear very close to the diagonal, as shown in Figs. 5(a) and 5(b). The area close to the filled diagonal shows an energy landscape of barriers and minima in the first and second neighboring lattice points. The extra particle is favored to sit on one of these minima and the energy is $E_p=-5.7163$. This energy is very close to the value corresponding to the situation when the particle is placed very far from the diagonal (then $E_p=-5.7160$), and much lower than when the particle is placed at the barrier (where $E_p=-5.7109$).

Additional particles will favor the creation of a second stripe, parallel to the existing one, either very far, so that there is no interaction, or very close, so that the particles of one stripe are located in the energy minima created by the other. When we place the particles in any other arrangement, the energy we find is higher.

IV. DISCUSSION

In this paper we have considered the interaction of a quantum particle with an elastic medium with strain coupled to the electronic density, in contrast to the usual Holstein polaron problem in which the displacement couples to the density. The three principal strain modes, dilatational e_1, compression shear e_2, and simple shear e_3, together with the strain compatibility condition, lead to a long-range anisotropic interaction. The lattice interaction with the particle creates a deformation in the fields, and a bound state is formed with energy lower than the extended plane-wave solutions (i.e., the delocalized polaron state). Due to the symmetry of the fields, an angular dependence is expected both in the elastic fields and the particle probability distribution. We find that the angular dependence of the probability distribution is much weaker than the exponential localization, unlike the anisotropy in the elastic fields. Thus the quasiparticle has a local electronic core with long-range, anisotropic elastic fields. For e_1, we see the fourfold symmetry of the square, and, depending on the ratio of the elastic stiffnesses A_2/A_3, there is a rotation by $\pi/4$ in the maxima and the minima of this field. This is consistent with an analysis of the dependence on orientation in Eq. (10).

We have extended the model to study the many polaron problem, where we also introduce a hard-core repulsion between polarons. There is an indirect long-range interaction between the polarons due to the long-range nature of the elastic fields, and the angular dependence of the fields affects the orientation of the interaction. We have calculated the interaction energy as a function of the relative position of two polarons and find that there are four minima along the diagonals of the lattice if $A_3<2A_2$, or along the main lattice directions for $A_3>2A_2$ (together with energy barriers along the other directions). The minima and barriers appear due to the constructive or destructive overlap of the deformations of the elastic fields created by the two polarons as they follow the fourfold symmetry of the e_1 field. Next, we studied the interaction of three polarons by placing two of them along the diagonal (in the minima) and then calculating the energy of the system as a function of the relative position of the third polaron. We found that the minima along the first diagonal (defined by the first two polarons) are amplified, whereas the

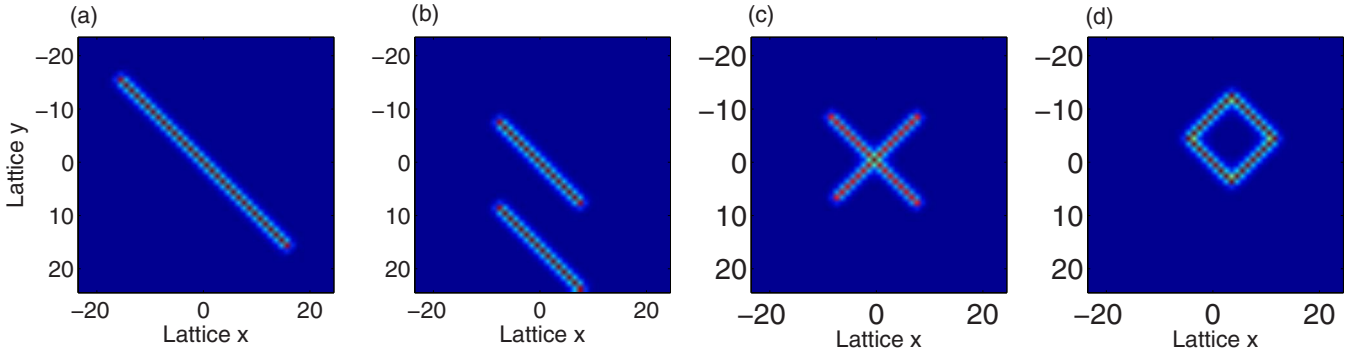

FIG. 6. (Color online) Configurations of polarons (their energy per particle is given in Table I) illustrating that for relatively small numbers of polarons, the angular dependence of the strain field favors diagonal strings.

minima along the other diagonal are weakened. The constructive overlap of the deformations of the e_1 field creates a preferred direction for the placement of many polarons. For a large number of polarons in the system, the minimum in the energy occurs if they are placed in a line (diagonal or main lattice direction, depending on the ratio A_2/A_3), following the symmetry of the field e_1. This favors the formation of strings or stripes in a many-polaron system similar to those observed in doped metal transition oxides.[9]

ACKNOWLEDGMENTS

This research was carried out under the auspices of the National Nuclear Security Administration of the U.S. Department of Energy at Los Alamos National Laboratory under Contract No. DE-AC52-06NA25396. We are grateful to S. R. Shenoy and R. Groger for many stimulating discussions.

[1] *Nanoscale Phase Separation and Colossal Magnetoresistance*, edited by E. Dagotto (Springer-Verlag, Berlin, 2003).
[2] *Intrinsic Multiscale Structure and Dynamics in Complex Electronic Oxides*, edited by A. R. Bishop, S. R. Shenoy, and S. Sridhar (World Scientific, Singapore, 2003).
[3] A. R. Bishop, T. Lookman, A. Saxena, and S. R. Shenoy, Europhys. Lett. **63**, 289 (2003).
[4] K. H. Ahn, T. Lookman, and A. R. Bishop, Nature (London) **428**, 401 (2004).
[5] T. Kimura, T. Goto, N. Shintani, K. Ishizaka, T. Arima, and Y. Tokura, Nature (London) **426**, 55 (2003).
[6] N. Mathur and P. Littlewood, Phys. Today **56** (1), 25 (2003); *Colossal Magnetoresistance and Related Properties*, edited by B. Raveau and C. N. R. Rao (World Scientific, Singapore, 1998).
[7] H. Y. Hwang, T. T. M. Palstra, S. W. Cheong, and B. Batlogg, Phys. Rev. B **52**, 15046 (1995).
[8] M. Fäth, S. Friesem, A. A. Menovsky, Y. Tomioka, J. Aarts, and J. A. Mydosh, Science **285**, 1540 (1999).
[9] V. J. Emery and S. A. Kivelson, Physica C **235**, 189 (1994).
[10] *Polarons and Bipolarons in High T_c Superconductors*, edited by E. K. H. Salje, A. S. Alexandrov, and W. Y. Liang (Cambridge University Press, Cambridge, UK, 1995).
[11] F. Kusmartsev, Phys. Rev. Lett. **84**, 5026 (2000).
[12] D. I. Khomskii and K. I. Kugel, Europhys. Lett. **55**, 208 (2001).
[13] G. Kalosakas, S. Aubry, and G. P. Tsironis, Phys. Rev. B **58**, 3094 (1998).
[14] P. Maniadis, G. Kalosakas, K. Ø. Rasmussen, and A. R. Bishop, Phys. Rev. B **68**, 174304 (2003).
[15] N. K. Voulgarakis and G. P. Tsironis, Phys. Rev. B **63**, 014302 (2000).
[16] T. Lookman, S. R. Shenoy, K. Ø. Rasmussen, A. Saxena, and A. R. Bishop, Phys. Rev. B **67**, 024114 (2003); S. R. Shenoy, T. Lookman, A. Saxena, and A. R. Bishop, *ibid.* **60**, R12537 (1999).
[17] R. Groger, T. Lookman, and A. Saxena, arXiv:0806.4564, Phys. Rev. B (to be published).